



Published in final edited form as:

*Mol Psychiatry*. 2014 August ; 19(8): 915–922. doi:10.1038/mp.2014.46.

## Evolutionarily-conserved prefrontal-amygdalar dysfunction in early-life anxiety

Rasmus M. Birn, Ph.D.<sup>a,b,e,f,g,\*</sup>, Alexander J. Shackman, Ph.D.<sup>h,i,j,\*</sup>, Jonathan A. Oler, Ph.D.<sup>b,e,f</sup>, Lisa E. Williams, Ph.D.<sup>b,e,f</sup>, Daniel R. McFarlin, Ph.D.<sup>b,e,f,g</sup>, Gregory M. Rogers, Ph.D.<sup>b</sup>, Steven E. Shelton, B.S.<sup>b</sup>, Andrew L. Alexander, Ph.D.<sup>a,g</sup>, Daniel S. Pine, MD<sup>k</sup>, Marcia J. Slattery, MD<sup>b</sup>, Richard J. Davidson, Ph.D.<sup>b,c,d,e,g</sup>, Andrew S. Fox, Ph.D.<sup>b,c,d,e,f,g</sup>, and Ned H. Kalin, MD<sup>b,c,e,f,g</sup>

<sup>a</sup>Department of Medical Physics, University of Wisconsin, Madison, WI 53719 USA

<sup>b</sup>Department of Psychiatry, University of Wisconsin, Madison, WI 53719 USA

<sup>c</sup>Department of Psychology, University of Wisconsin, Madison, WI 53719 USA

<sup>d</sup>Center for Investigating Healthy Minds, University of Wisconsin, Madison, WI 53719 USA

<sup>e</sup>HealthEmotions Research Institute, University of Wisconsin, Madison, WI 53719 USA

<sup>f</sup>Lane Neuroimaging Laboratory, University of Wisconsin, Madison, WI 53719 USA

<sup>g</sup>Waisman Laboratory for Brain Imaging and Behavior, University of Wisconsin, Madison, WI 53719 USA

<sup>h</sup>Department of Psychology, University of Maryland, College Park, MD 20742 USA

<sup>i</sup>Neuroscience and Cognitive Science Program, University of Maryland, College Park, MD 20742 USA

<sup>j</sup>Maryland Neuroimaging Center, University of Maryland, College Park, MD 20742 USA

<sup>k</sup>Section on Development and Affective Neuroscience, National Institute of Mental Health, Bethesda, MD, 20892 USA

### Abstract

Users may view, print, copy, and download text and data-mine the content in such documents, for the purposes of academic research, subject always to the full Conditions of use:[http://www.nature.com/authors/editorial\\_policies/license.html#terms](http://www.nature.com/authors/editorial_policies/license.html#terms)

Address Manuscript Correspondence to: Ned H. Kalin (nkalin@wisc.edu), HealthEmotions Research Institute, Wisconsin Psychiatric Institute & Clinics, University of Wisconsin—Madison, 6001 Research Park Boulevard, Madison, Wisconsin 53719 USA.

\*Contributed equally to this work

Authors declare no conflicts of interest.

**Contributions:** N.H.K., J.A.O., D.S.P., M.J.S., and S.E.S. designed the study. S.E.S. collected monkey data. L.E.W. collected human data. A.L.A. optimized imaging methods. D.S.P., N.H.K., and G.M.R. made childhood psychiatric diagnoses. R.M.B. and A.S.F. developed analytical tools. R.M.B., J.A.O., A.J.S., and A.S.F. performed data processing for monkey data. D.R.M., L.E.W., J.A.O., A.J.S., and R.M.B. performed data processing for human data. R.M.B., A.J.S., J.A.O., and N.H.K. analyzed monkey data. D.R.M., L.E.W., J.A.O., A.J.S., R.M.B., and N.H.K. analyzed human data. A.J.S., N.H.K., R.M.B., A.S.F., J.A.O., R.J.D., and D.S.P. interpreted data. A.J.S., A.S.F., N.H.K., J.A.O., L.E.W., and R.M.B. wrote the paper. A.J.S., A.S.F., and N.H.K. created the figures. A.J.S., J.A.O., and L.E.W. created the tables. N.H.K. supervised the study. All authors contributed to revising the paper.

Supplementary information (SI) is available at *Molecular Psychiatry's* website.

Some individuals are endowed with a biology that renders them more reactive to novelty and potential threat. When extreme, this anxious temperament (AT) confers elevated risk for the development of anxiety, depression, and substance abuse. These disorders are highly prevalent, debilitating, and can be challenging to treat. The high-risk AT phenotype is expressed similarly in children and young monkeys and mechanistic work demonstrates that the central nucleus (Ce) of the amygdala is an important substrate. While it is widely believed that the flow of information across the structural network connecting the Ce to other brain regions underlies primates' capacity for flexibly regulating anxiety, the functional architecture of this network has remained poorly understood. Here we used functional magnetic resonance imaging (fMRI) in anesthetized young monkeys and quietly resting children with anxiety disorders to identify an evolutionarily-conserved pattern of functional connectivity relevant to early-life anxiety. Across primate species and levels of awareness, reduced functional connectivity between the dorsolateral prefrontal cortex (dlPFC), a region thought to play a central role in the control of cognition and emotion, and the Ce was associated with increased anxiety assessed outside the scanner. Importantly, high-resolution 18-fluorodeoxyglucose positron emission tomography (FDG-PET) imaging provided evidence that elevated Ce metabolism statistically mediates the association between prefrontal-amygdalar connectivity and elevated anxiety. These results provide new clues about the brain network underlying extreme early-life anxiety and set the stage for mechanistic work aimed at developing improved interventions for pediatric anxiety.

### Keywords

amygdala; behavioral inhibition (BI); developmental psychopathology; multimodal brain imaging; pediatric anxiety; resting-state fMRI

### Introduction

Some children and animals characteristically show heightened reactions to novelty and potential threat<sup>1-2</sup>. When extreme, this anxious temperament (AT) is a well-established risk factor for the development of anxiety, depression, and comorbid substance abuse<sup>3-4</sup>. These disorders are common, debilitating, and difficult to treat<sup>5-7</sup>. As such, they represent a growing burden on public healthcare systems and an important challenge for clinicians, health economists, and public policy-makers<sup>8-9</sup>. AT is a trait-like phenotype that is determined by a combination of heritable and non-heritable factors, evident early in life, and characterized by increased behavioral and hypothalamic-pituitary-adrenal (HPA) reactivity to novelty and potential threat<sup>3, 10-13</sup>. There is considerable evidence that the high-risk AT phenotype is attenuated by anxiolytic compounds<sup>14-15</sup> and expressed similarly in children and young monkeys<sup>3, 10</sup>. Importantly, mechanistic and neuroimaging studies in young monkeys demonstrate that metabolic activity in the central nucleus (Ce) of the amygdala is a key substrate for individual differences in early-life AT. In particular, selective excitotoxic lesions of the primate Ce reduce AT<sup>16</sup>, consistent with studies of human patients with circumscribed amygdala damage<sup>17</sup>. Furthermore, in young monkeys individual differences in Ce metabolism are trait-like and predict substantial variation in the AT phenotype<sup>10-13</sup>. These observations are in accord with evidence that the Ce can initiate a broad spectrum of

defensive responses via efferent projections to the brain regions that directly mediate many of the behavioral, physiological, and cognitive features of anxiety<sup>11, 18-19</sup>.

There is consensus that neuropsychiatric disorders, like other complex mental processes, reflect alterations in the coordinated activity of distributed functional circuits<sup>20</sup>. Anatomically, the Ce is embedded in a complex web of monosynaptically and polysynaptically connected brain regions<sup>19</sup>. This structural backbone encompasses a number of cortical regions that are especially well-developed in primates, including the anterior cingulate cortex (ACC), insula, and prefrontal cortex (PFC)<sup>21-23</sup>. While it widely believed that the synchronized flow of information across this network underlies primates' capacity for flexibly regulating anxiety, the functional architecture of the Ce network and its relevance to early-life anxiety remains poorly understood. This partially reflects the fact that functional networks need not recapitulate the direct structural connections revealed by traditional tract tracing techniques<sup>24-25</sup>. In particular, there is mounting evidence that regulatory signals can propagate across more complex, indirect pathways<sup>26</sup>.

Here, we used a combination of neuroimaging modalities to survey the entire brain for patterns of functional connectivity predictive of both the intermediate brain phenotype (Ce metabolism) and the high-risk phenotype (AT). Specifically, we used functional magnetic resonance imaging (fMRI) and high-resolution <sup>18</sup>fluorodeoxyglucose positron emission tomography (FDG-PET) to first trace the intrinsic functional connectivity of the Ce in anesthetized young monkeys and then to identify connectivity patterns associated with Ce metabolism and anxiety. fMRI-derived measures of intrinsic functional connectivity are particularly useful because they are sensitive to functional networks spanning polysynaptic circuits<sup>27-29</sup>, just as viral tracers can be used to delineate polysynaptic structural pathways<sup>30</sup>. Indeed, there is ample evidence of robust functional connectivity between brain regions that lack direct structural connections<sup>28-29, 31</sup>. This is critical because the Ce is the major output region of the amygdala and receives relatively few direct projections from prefrontal regions implicated in the regulation of stress and anxiety<sup>19, 32-34</sup>. Therefore, the regulation of Ce activity is likely to be mediated indirectly, via polysynaptic circuits spanning the prefrontal cortex (PFC) and neighboring regions of the amygdala with the capacity to convey cortical regulatory signals to the Ce<sup>19, 32-33</sup>. Finally, to assess the relevance of our discoveries in the rhesus monkey to understanding childhood disease, we used fMRI to search for homologous patterns of intrinsic functional connectivity in children with anxiety disorders. Identifying an evolutionary conserved functional circuit relevant to extreme anxiety would reinforce the validity of the young rhesus model and set the stage for future mechanistic research aimed at understanding the origin of differences in the strength of functional connectivity<sup>35-36</sup>.

## Methods

Except where noted otherwise, behavioral and brain imaging methods have been described in detail in prior publications and are only briefly summarized<sup>10-13, 37</sup>. Additional details are provided in the SI.

## Subjects

**Young monkeys**—Eighty-nine periadolescent monkeys (*Macaca mulatta*; median (*SD*) age=2.69 (.97) years; 54% female) were phenotyped and brain imaged. This sample represents the subset of monkeys previously described by our group with complete multimodal imaging datasets (FDG-PET:  $n=238$ ; fMRI:  $n=107$ )<sup>11-12, 37</sup>.

**Children**—Twenty-eight children (8-12 years) who met standard inclusion and exclusion criteria (see the SI) were enrolled: 14 patients with a current pediatric anxiety disorder (mean age (*SD*)=9.9 (1.2) years) and 14 demographically-matched, psychiatrically-healthy controls (mean age (*SD*)=10.2 (1.3) years). Patients met criteria for one or more current pediatric anxiety disorders, including Generalized Anxiety Disorder, Separation Anxiety Disorder, Social Phobia, or Anxiety Disorder Not Otherwise Specified. Children were recruited from local psychiatric clinics via clinician referral and from the community via media advertisements. The groups did not differ in age or sex (4 females/group). Prior to the MRI scan, anxiety diagnoses were confirmed by a Ph.D.-level clinical psychologist using the Kiddie-Schedule for Affective Disorders and Schizophrenia Present and Lifetime versions (KSADS-PL)<sup>38</sup>. At the time of the MRI session, 4 patients were receiving psychotropic medications (see the SI). Control children had no known history of mental illness (see the SI).

## Data Acquisition and Processing

**Young monkeys**—T1-weighted structural and T2\*-weighted echo-planar imaging (EPI) functional MRI data were collected under anesthesia. As detailed in the SI, EPI data were processed using standard techniques in AFNI (<http://afni.nimh.nih.gov>) except where noted otherwise. Data were processed to attenuate motion artifact, field distortions, physiological noise, and slice-timing differences. To further attenuate physiological noise, average white matter and cerebrospinal fluid time-series and their temporal derivatives were residualized from the EPI time series. EPI volumes with >1mm of motion (see the SI) were censored from data analyses. Using this criterion, no volumes were censored for any of the young monkeys.

In a separate session, monkeys received <sup>18</sup>F<sub>2</sub> immediately prior to the 30-minute No-Eye Contact (NEC) challenge used to elicit the AT phenotype<sup>10-13</sup> (median (*SD*) intersession interval=21.0 (42.4) days). Subjects were placed in a standard testing cage. An experimenter entered the room and stood motionless ~2.5 meters from the subject while presenting his profile and avoiding direct eye contact. Subjects were allowed to freely respond to this ethologically-relevant potential threat, similar to procedures used to assay dispositional anxiety and behavioral inhibition in children<sup>2-3</sup>. Increases in freezing and decreases in vocalizations were quantified by an experienced observer. Following behavioral testing, plasma was collected for quantifying cortisol and subjects were anesthetized and positioned in the PET scanner. Higher FDG-PET signals reflect greater regional metabolism (i.e., increased FDG uptake) during the preceding NEC challenge. FDG-PET, which provides a measure of regional brain metabolism integrated over the entire 30-minute behavioral challenge, is ideally suited for assessing trait-like neural activity. AT was computed as the

mean of standardized plasma cortisol, freezing, and reverse-scored vocalizations in response to the human intruder's profile (30-min).

**Children**—Prior to scanning, children completed a mock MRI session, which has been shown to improve data quality in pediatric neuroimaging applications<sup>39</sup>. MRI data were collected using a standard 8-channel head coil. Anatomical scans were obtained with a 3D T1-weighted, inversion-recovery, fast gradient-echo prescription (TI/TR/TE/Flip/NEX/FOV/Matrix/Bandwidth: 450ms/8.16ms/3.18ms/12°/1/256mm/256×256/31.25kHz) with whole brain coverage (156 slices over 156 mm). Functional scans were obtained using a 2D T2\*-weighted EPI prescription (TR/TE/Flip/FOV/Matrix: 2000ms/25ms/60°/240mm/64×64; 40×4.0-mm sagittal slices; gap: 0 mm; 180 volumes). Subjects were instructed to remain motionless while remaining relaxed and awake.

Except where noted otherwise, procedures were identical to those employed in the young nonhuman primate sample. Native-space T1 images were nonlinearly registered to the MNI probabilistic template (MNI152\_T1\_1mm\_brain; <http://fsl.fmrib.ox.ac.uk>) using FLIRT and FNIRT from FSL<sup>40-42</sup>. Single-subject EPI data were spatially normalized using the resulting transformation matrices and re-sampled to 2-mm isotropic voxels. Normalized EPI data were spatially smoothed (6mm FWHM). Datasets were visually inspected to ensure adequate EPI coverage without excess susceptibility or distortion. The two groups did not significantly differ in the mean amount of motion or fraction of uncensored data,  $p>.48$ ,  $df=26$  (see the SI).

## Hypothesis Testing

**Young monkeys**—A previously validated seed-based approach was used to identify the Ce functional network (see Fig. S1 and Table S1 for additional validation analyses)<sup>37</sup>. Given our focus on AT-related Ce metabolism, the seed was functionally defined as the 95% spatial confidence interval surrounding the Ce voxel where FDG metabolism most strongly predicted AT in a superset of 238 individuals (turquoise region in Fig. 1a; see Ref. <sup>12</sup>). Importantly, in prior work we used *in vivo* chemoarchitectonic techniques to demonstrate that this functionally-defined region corresponds to the sub-region of the primate amygdala where excitotoxic lesions attenuate anxiety<sup>12, 16, 37</sup>, a degree of precision that is difficult to achieve using conventional imaging techniques in humans (e.g., Refs. <sup>43, 44</sup>). As in other recent work by our group<sup>43-44</sup>, hypothesis testing employed statistical maps that were thresholded ( $p=.05$ , corrected) based on cluster extent. Null distributions were estimated via Monte Carlo simulations (50,000 iterations; *3dClustSim*). Simulations incorporated the mean spatial smoothness of the single-subject residuals, estimated using  $3dFWHMx$ , and an uncorrected voxelwise threshold of  $p=.005$ . All hypothesis-testing analyses controlled for nuisance variation in mean-centered age and sex.

We used a standard multivariate analytic framework<sup>45-46</sup> to test whether the relationship between prefrontal-amygdalar functional connectivity and AT is statistically mediated by Ce metabolism (Connectivity → Metabolism → AT). As with our other analyses, we controlled for nuisance variance in mean-centered age and sex. For recent applications of this framework to neuroimaging datasets, see Refs. <sup>11, 47-48</sup>. Satisfying the criteria of this

framework would demonstrate that a significant proportion of the association between prefrontal-Ce connectivity and AT is explained by metabolism, an inference not afforded by simpler bivariate tests. Operationally, mediation required four significant tests: **(a)** Connectivity  $\rightarrow$  Metabolism, **(b)** Connectivity  $\rightarrow$  AT, **(c)** Metabolism  $\rightarrow$  AT, and **(d)** controlling for variation in Metabolism significantly weakens the Connectivity  $\rightarrow$  AT correlation. Consistent with our prior work<sup>11, 49</sup>, the final criterion was assessed using Clogg's test<sup>45, 50</sup> conservatively thresholded at  $p < .05$  (Sidak-corrected for the total volume of the regions where connectivity predicted both Ce metabolism and AT;  $df = n - 3$  - number of covariates). This test does *not* provide evidence of causation and more complex alternative pathways cannot be rejected.

**Children**—Imaging data were processed using the same techniques employed with the nonhuman primate sample. Here, the Ce seed was anatomically defined using well-established techniques (see the SI)<sup>37</sup>. Using this seed, we tested whether children with anxiety disorders and extremely anxious young monkeys show a similar pattern of Ce functional connectivity.

## Results

### Young Monkeys

Whole-brain regression analyses revealed several prefrontal and subcortical regions with significant Ce functional connectivity ( $p < 5.0 \times 10^{-9}$ , uncorrected;  $df = 86$ ; Fig. 1b and Table S2). These clusters encompassed regions that project to the Ce, such as the pregenual anterior cingulate cortex (pgACC), and regions that receive projections from the Ce, such as the bed nucleus of the stria terminalis (BNST)<sup>19, 32, 37, 51-53</sup>. Other clusters encompassed regions that appear to lack direction connections with the Ce, including the dorsolateral prefrontal cortex (dlPFC) and subgenual anterior cingulate cortex (sgACC)<sup>19, 32, 37, 51-53</sup>.

Next, we searched the entire brain for functional connections, indexed using fMRI, that are predictive of Ce metabolism, indexed using FDG-PET. This revealed that increased Ce metabolism was associated with decreased functional connectivity between the Ce and two prefrontal regions, mPFC and right dlPFC ( $p < .05$ , whole-brain corrected;  $df = 85$ ; Fig. 2 and Table S3). The mPFC cluster encompassed several architectonically-distinct regions, including pgACC (area 32), frontopolar cortex (area 10M), and medial orbitofrontal cortex (OFC; area 14M; see Fig. S2). Together, the dlPFC-Ce and mPFC-Ce functional networks statistically explained 22% of the variance in Ce metabolism ( $F(2,84) = 5.92$ ,  $p < .001$ , uncorrected).

We also tested whether variation in intrinsic functional connectivity between these prefrontal regions and the Ce predicts AT. Paralleling the metabolism results (Fig. 2), young monkeys with higher levels of the anxious phenotype showed decreased functional connectivity between the Ce and both the medial and dorsolateral PFC clusters ( $p < .05$ , corrected; Fig. 3a; Table S4; Fig. S3). This indicates that functional connectivity measured under anesthesia is associated with objective differences in threat-elicited defensive behaviors and neuroendocrine activity assessed outside of the scanner environment. Exploratory analyses indicated that these relations were significant for each constituent of

the composite AT phenotype (standardized freezing, vocalizations, and cortisol:  $prs = -.25$  to  $-.32$ , uncorrected  $ps < .03$ ;  $df = 85$ ). Collectively, variation in the strength of connectivity between the Ce and these two prefrontal regions accounted for 23% of the variation in AT ( $F(2,84) = 7.29$ ,  $p < .001$ , uncorrected).

Finally, we tested whether the association between prefrontal-Ce functional connectivity and the anxious phenotype is statistically mediated by Ce metabolic activity (i.e., prefrontal-Ce connectivity  $\rightarrow$  Ce metabolism  $\rightarrow$  AT), as one would expect given evidence that the Ce is a mechanistically-important proximal substrate of the anxious phenotype<sup>16</sup>. We first confirmed that Ce metabolism predicts AT in the present sample ( $t = 6.70$ ,  $p = 2.3 \times 10^{-9}$ , uncorrected;  $df = 85$ ; Fig. 3b), consistent with our prior report<sup>12</sup>. Critically, the statistical mediation test was also significant for both the dlPFC-Ce and mPFC-Ce networks, indicating that variation in Ce metabolism explains a significant proportion of the association between prefrontal-Ce functional connectivity and AT ( $ps < .05$ , corrected;  $df = 84$ ; Figs. 3c and S3, Table S4). These effects were specific; control analyses demonstrated that mediation effects were not significant for alternative network models (i.e., Ce metabolism  $\rightarrow$  prefrontal-Ce connectivity  $\rightarrow$  AT;  $ts < 2.52$ ,  $ps > .05$ , corrected;  $df = 84$ ). Taken together, these findings are consistent with the possibility that the association between prefrontal-Ce functional connectivity (i.e., mPFC-Ce and dlPFC-Ce) and dispositional anxiety reflects prefrontal influences on Ce metabolism, presumably supported by polysynaptic structural pathways. Importantly, control analyses indicated that individual differences in functional connectivity, Ce metabolism, and AT were not significantly associated with variation in motion artifact, uncorrected  $ps > .24$ ,  $df = 85$  (see the SI).

## Children

Our results indicate that young monkeys with extreme AT are characterized by decreased functional connectivity between the PFC and Ce under anesthesia. Next, we tested whether a similar pattern is evident in quietly resting children with anxiety disorders. In fact, patients showed decreased functional connectivity between the dlPFC and Ce compared to healthy control subjects ( $p < .05$ , when corrected for the combined volume of the dlPFC and mPFC;  $df = 24$ ; n.s. when corrected for the volume of the entire brain; Fig. 4a, Figs. S5-S6, and Table S5). Significant effects were not obtained for the mPFC-Ce network in the pediatric anxiety sample. Accordingly, in the remainder of the report we focus on the evolutionarily-conserved dlPFC-Ce functional network. Follow-up analyses revealed that the reduction in dlPFC-Ce connectivity evident in the pediatric patients remained significant after controlling for age and sex (Table S5), controlling for individual differences in motion (see the SI), or excluding 4 medicated patients (see the SI). Collectively, these results demonstrate that decreased functional connectivity between the dlPFC and Ce is associated with extreme anxiety outside the imaging environment in both quietly resting children and anesthetized young monkeys (Fig. 4a-b). The consistency of this relationship across species and levels of awareness at the time of scanning makes it unlikely that it reflects either a sedation artifact or differences in stress elicited by the scanner environment.

## Discussion

The present results provide evidence that extreme anxiety early in life is associated with evolutionarily-conserved alterations in the strength of intrinsic functional connectivity between the dlPFC and Ce. Among both children and monkeys, individuals with low levels of connectivity were characterized by high levels of anxiety when assessed outside of the scanner environment (Figs. 2 and 4), raising the possibility that chronically altered functional coordination between these regions contributes to the development of pathological anxiety. In the larger sample of young monkeys, decreased functional connectivity with the dlPFC as well as the mPFC was associated with elevated metabolism in the Ce, a mechanistically-important substrate for trait-like differences in anxiety<sup>12, 16</sup>.

In children, AT is a well-established risk factor for the development of anxiety and other psychiatric disorders<sup>3-4</sup> and our results provide a novel framework for understanding the mechanisms underlying this liability. Prior work suggests that Ce metabolism underlies much of the experience-dependent risk that contributes to the development of extreme anxiety<sup>12-13</sup>. Likewise, recent work suggests that prefrontal-amygdalar functional connectivity can be influenced by early adversity<sup>43-44</sup>. This plasticity suggests that interventions targeting either Ce metabolism or the larger functional circuit in which it is embedded may prove to be effective strategies for reducing anxiety in children who, because of their extreme temperament, are at increased risk for developing psychopathology. By virtue of its well-established capacity for regulating mood, attention, memory, and action<sup>34, 54-56</sup>, the dlPFC is well-positioned to translate early-life experiences into enduring alterations in Ce function.

Given the absence of established direct projections, the association between dlPFC-Ce functional connectivity and early-life anxiety is presumably supported by a polysynaptic structural network. While our results do not identify the precise constituents of this circuit, there is growing mechanistic evidence that the PFC can influence information processing in distal brain regions via biasing signals that propagate across polysynaptic structural pathways<sup>26, 57-58</sup>. This network could reflect either undiscovered projections<sup>59, 60</sup> or established projections from the dlPFC to neighboring regions of the dorsal amygdala, such as the magnocellular division of the basal nucleus (Bmc), that are strongly interconnected with the Ce. In particular, the dlPFC projects to a region of the dorsal Bmc that lies within a few millimeters of the Ce<sup>19, 51-53</sup>, a difference that cannot be resolved using conventional fMRI techniques (see the SI).

Analyses of data obtained from the larger nonhuman primate sample revealed that Ce metabolism statistically mediates the association between prefrontal-amygdalar connectivity and AT, suggesting that Ce metabolic activity represents an intermediate link between intrinsic functional connectivity and chronically elevated anxiety (i.e., decreased prefrontal-Ce connectivity → increased Ce metabolism → increased anxiety; Fig. 3). Notably, this pattern was evident for functional connectivity between the Ce and two regions of the PFC: dlPFC and mPFC. While our results do not provide evidence that the mPFC-Ce is evolutionarily conserved, this may reflect insufficient power in the pediatric anxiety sample. Other work highlights the potential importance of the mPFC-Ce functional network. For

example, reduced functional connectivity between the mPFC and amygdala has been shown to predict heightened dispositional anxiety in several human imaging studies<sup>59-60</sup>. The present results suggest that this association between connectivity and anxiety stems from chronically elevated metabolic activity in the Ce.

Clearly, important challenges remain. As with other brain imaging studies, our analyses do not permit mechanistic inferences and alternative causal pathways are possible. Like other studies focused on measures of functional connectivity, our conclusions are tempered by questions about the origins and significance of correlated fluctuations in the blood-oxygen-level dependent (BOLD) fMRI signal<sup>61-63</sup>. Furthermore, while it is clear from lesion studies that the Ce is mechanistically involved in AT<sup>16</sup>, we cannot reject the possibility that both increased anxiety and reduced prefrontal functional connectivity reflect symptoms of chronically elevated Ce metabolism. In particular, the Ce is well-positioned to influence the signal-to-noise ratio (SNR) of information processing in the PFC<sup>64-67</sup>, via projections to diffuse neuromodulatory systems in the basal forebrain and striatum. Dampened prefrontal SNR would tend to manifest as reduced functional connectivity<sup>68</sup>. A key challenge for future studies will be to use mechanistic techniques in nonhuman primates to adjudicate between these alternatives and to more fully delineate the polysynaptic circuit supporting correlated activity in the dlPFC and Ce. Combined with fMRI, transcranial magnetic stimulation represents a noninvasive alternative strategy that could be applied in humans<sup>69-70</sup>. It will also be important to test whether existing anxiolytic compounds rescue dlPFC-Ce functional connectivity. If so, then this biomarker could potentially be used to evaluate novel therapeutics<sup>36, 71</sup>. Finally, it will be useful to more fully evaluate whether aberrant dlPFC-Ce functional connectivity is a transdiagnostic feature of the anxiety disorders and whether it represents a substrate for childhood AT or related constructs, such as behavioral inhibition and shyness, that were not assessed in the pediatric sample.

## Conclusions

Existing treatments for anxiety disorders are inconsistently effective or associated with significant adverse effects<sup>5, 7</sup>, highlighting the need to identify and understand the neural mechanisms that confer risk. Building on prior mechanistic and neuroimaging work, the present study demonstrates that extreme anxiety is associated with reduced functional connectivity between the dlPFC and Ce in anesthetized young monkeys and quietly resting children. Translational brain imaging strategies, like that featured in the present report, provide a powerful tool for closing the gap separating the mechanistic insights afforded by nonhuman animal models from the complexity of human psychopathology and accelerating the pace of therapeutic development<sup>35-36</sup>. Our results also indicate that the association between prefrontal-amygdalar connectivity and anxiety is statistically mediated by Ce metabolism. Importantly, these results are fundamentally grounded in psychiatrically-important emotional behaviors. For example, differences in the strength of prefrontal-Ce functional connectivity were found to predict anxiety-related behaviors (i.e., behavioral inhibition) and cortisol elicited by an ethologically-relevant threat in freely-behaving young monkeys. The use of a relatively large discovery sample, functionally- and mechanistically-defined seed region, well-validated primate model of pediatric anxiety, and clinical confirmatory sample enhances confidence in the translational significance of these results<sup>72</sup>.

More broadly, the present study provides unique evidence that early-life temperament does not just reflect differences in neural reactivity to trait-relevant cues (e.g., the amygdala's threshold to respond or peak response to threat<sup>2, 73</sup>), but is also embodied in the intrinsic activity of the brain.

## Supplementary Material

Refer to Web version on PubMed Central for supplementary material.

## Acknowledgments

Authors acknowledge the assistance of E. Ahlers, V. Balchen, B. Christian, A. Converse, L. Friedman, M. Jesson, E. Larson, K. Mayer, T. Oakes, M. Riedel, P. Roseboom, J. Storey, D. Tromp, N. Vack, H. Van Valkenberg, and the staffs of the Harlow Center for Biological Psychology, HealthEmotions Research Institute (HERI), Waisman Center, Waisman Laboratory for Brain Imaging and Behavior, and Wisconsin National Primate Center. This work was supported by the National Institutes of Health (NIH; Intramural Research Program and extramural grants HD003352, HD008352, MH018931, MH046729, MH081884, MH084051, MH090912, MH091550, OD011106, and RR000167), HERI, Meriter Hospital, and the University of Maryland.

## References

1. Darwin, C. The expression of the emotions in man and animals. 4th. Oxford University Press; NY: 1872/2009.
2. Kagan J, Reznick JS, Snidman N. Biological bases of childhood shyness. *Science*. 1988; 240:167–171. [PubMed: 3353713]
3. Fox NA, Henderson HA, Marshall PJ, Nichols KE, Ghera MM. Behavioral inhibition: linking biology and behavior within a developmental framework. *Annu Rev Psychol*. 2005; 56:235–262. [PubMed: 15709935]
4. Blackford JU, Pine DS. Neural substrates of childhood anxiety disorders: a review of neuroimaging findings. *Child Adolesc Psychiatr Clin N Am*. 2012; 21:501–525. [PubMed: 22800991]
5. Bystritsky A. Treatment-resistant anxiety disorders. *Mol Psychiatry*. 2006; 11:805–814. [PubMed: 16847460]
6. Kessler RC, Petukhova M, Sampson NA, Zaslavsky AM, Wittchen HU. Twelve-month and lifetime prevalence and lifetime morbid risk of anxiety and mood disorders in the United States. *Int J Methods Psychiatr Res*. 2012; 21:169–184. [PubMed: 22865617]
7. Cloos JM, Ferreira V. Current use of benzodiazepines in anxiety disorders. *Curr Opin Psychiatry*. 2009; 22(1):90–95. [PubMed: 19122540]
8. Collins PY, Patel V, Joestl SS, March D, Insel TR, Daar AS, et al. Grand challenges in global mental health. *Nature*. 2011; 475:27–30. [PubMed: 21734685]
9. Whiteford HA, Degenhardt L, Rehm J, Baxter AJ, Ferrari AJ, Erskine HE, et al. Global burden of disease attributable to mental and substance use disorders: findings from the Global Burden of Disease Study 2010. *Lancet*. in press.
10. Fox AS, Shelton SE, Oakes TR, Davidson RJ, Kalin NH. Trait-like brain activity during adolescence predicts anxious temperament in primates. *PLoS ONE*. 2008; 3:e2570. [PubMed: 18596957]
11. Shackman AJ, Fox AS, Oler JA, Shelton SE, Davidson RJ, Kalin NH. Neural mechanisms underlying heterogeneity in the presentation of anxious temperament. *Proc Natl Acad Sci U S A*. 2013; 110:6145–6150. [PubMed: 23538303]
12. Oler JA, Fox AS, Shelton SE, Rogers J, Dyer TD, Davidson RJ, et al. Amygdalar and hippocampal substrates of anxious temperament differ in their heritability. *Nature*. 2010; 466:864–868. [PubMed: 20703306]
13. Fox AS, Oler JA, Shelton SE, Nanda SA, Davidson RJ, Roseboom PH, et al. Central amygdala nucleus (Ce) gene expression linked to increased trait-like Ce metabolism and anxious

- temperament in young primates. *Proc Natl Acad Sci U S A*. 2012; 109:18108–18113. [PubMed: 23071305]
14. Kalin NH, Shelton SE, Turner JG. Effects of alprazolam on fear-related behavioral, hormonal, and catecholamine responses in infant rhesus monkeys. *Life Sci*. 1991; 49:2031–2044. [PubMed: 1660955]
  15. Kalin NH, Shelton SE. Defensive behaviors in infant rhesus monkeys: environmental cues and neurochemical regulation. *Science*. 1989; 243:1718–1721. [PubMed: 2564702]
  16. Kalin NH, Shelton SE, Davidson RJ. The role of the central nucleus of the amygdala in mediating fear and anxiety in the primate. *J Neurosci*. 2004; 24:5506–5515. [PubMed: 15201323]
  17. Feinstein JS, Adolphs R, Damasio A, Tranel D. The human amygdala and the induction and experience of fear. *Curr Biol*. 2011; 21:1–5. [PubMed: 21129968]
  18. Pare D, Duvarci S. Amygdala microcircuits mediating fear expression and extinction. *Curr Opin Neurobiol*. 2012; 22:717–723. [PubMed: 22424846]
  19. Freese, JL.; Amaral, DG. Neuroanatomy of the primate amygdala. In: Whalen, PJ.; Phelps, EA., editors. *The human amygdala*. Guilford; NY: 2009. p. 3-42.
  20. Uhlhaas PJ, Singer W. Neuronal dynamics and neuropsychiatric disorders: toward a translational paradigm for dysfunctional large-scale networks. *Neuron*. 2012; 75(6):963–980. [PubMed: 22998866]
  21. Shackman AJ, Salomons TV, Slagter HA, Fox AS, Winter JJ, Davidson RJ. The integration of negative affect, pain and cognitive control in the cingulate cortex. *Nat Rev Neurosci*. 2011; 12:154–167. [PubMed: 21331082]
  22. Preuss, TM. Primate brain evolution in phylogenetic context. In: Kaas, JH.; Preuss, TM., editors. *Evolution of Nervous Systems*. Vol. 4. Elsevier; NY: 2007. p. 3-34.
  23. Ongur D, Price JL. The organization of networks within the orbital and medial prefrontal cortex of rats, monkeys and humans. *Cereb Cortex*. 2000; 10:206–219. [PubMed: 10731217]
  24. Pessoa, L. *The cognitive-emotional brain: From interactions to integration*. MIT Press; Cambridge, MA: 2013.
  25. Pessoa L. Beyond brain regions: network perspective of cognition-emotion interactions. *Behav Brain Sci*. 2012; 35:158–159. [PubMed: 22617666]
  26. Ekstrom LB, Roelfsema PR, Arsenault JT, Bonmassar G, Vanduffel W. Bottom-up dependent gating of frontal signals in early visual cortex. *Science*. 2008; 321:414–417. [PubMed: 18635806]
  27. Buckner RL, Krienen FM, Yeo BT. Opportunities and limitations of intrinsic functional connectivity MRI. *Nat Neurosci*. 2013; 16:832–837. [PubMed: 23799476]
  28. Vincent JL, Patel GH, Fox MD, Snyder AZ, Baker JT, Van Essen DC, et al. Intrinsic functional architecture in the anaesthetized monkey brain. *Nature*. 2007; 447:83–86. [PubMed: 17476267]
  29. Honey CJ, Sporns O, Cammoun L, Gigandet X, Thiran JP, Meuli R, et al. Predicting human resting-state functional connectivity from structural connectivity. *Proc Natl Acad Sci U S A*. 2009; 106(6):2035–2040. [PubMed: 19188601]
  30. Dum RP, Levinthal DJ, Strick PL. The spinothalamic system targets motor and sensory areas in the cerebral cortex of monkeys. *J Neurosci*. 2009; 29:14223–14235. [PubMed: 19906970]
  31. Adachi Y, Osada T, Sporns O, Watanabe T, Matsui T, Miyamoto K, et al. Functional connectivity between anatomically unconnected areas is shaped by collective network-level effects in the macaque cortex. *Cereb Cortex*. 2012; 22(7):1586–1592. [PubMed: 21893683]
  32. Ghashghaei HT, Barbas H. Pathways for emotion: interactions of prefrontal and anterior temporal pathways in the amygdala of the rhesus monkey. *Neuroscience*. 2002; 115:1261–1279. [PubMed: 12453496]
  33. Stefanacci L, Amaral DG. Some observations on cortical inputs to the macaque monkey amygdala: an anterograde tracing study. *J Comp Neurol*. 2002; 451:301–323. [PubMed: 12210126]
  34. Buhle JT, Silvers JA, Wager TD, Lopez R, Onyemekwu C, Kober H, et al. Cognitive reappraisal of emotion: A meta-analysis of human neuroimaging studies. *Cereb Cortex*. in press.
  35. Casey BJ, Craddock N, Cuthbert BN, Hyman SE, Lee FS, Ressler KJ. DSM-5 and RDoC: progress in psychiatry research? *Nat Rev Neurosci*. 2013; 14(11):810–814. [PubMed: 24135697]

36. Borsook D, Becerra L, Hargreaves R. A role for fMRI in optimizing CNS drug development. *Nat Rev Drug Discov.* 2006; 5(5):411–424. [PubMed: 16604100]
37. Oler JA, Birn RM, Patriat R, Fox AS, Shelton SE, Burghy CA, et al. Evidence for coordinated functional activity within the extended amygdala of non-human and human primates. *Neuroimage.* 2012; 61:1059–1066. [PubMed: 22465841]
38. Kaufman J, et al. Schedule for Affective Disorders and Schizophrenia for School-Age Children—Present and Lifetime Version (K-SADS-PL): initial reliability and validity data. *J Am Acad Child Adolesc Psychiatry.* 1997; 36:980–988. [PubMed: 9204677]
39. de Bie HM, Boersma M, Wattjes MP, Adriaanse S, Vermeulen RJ, Oostrom KJ, et al. Preparing children with a mock scanner training protocol results in high quality structural and functional MRI scans. *Eur J Pediatr.* 2010; 169(9):1079–1085. [PubMed: 20225122]
40. Smith SM, Jenkinson M, Woolrich MW, Beckmann CF, Behrens TE, Johansen-Berg H, et al. Advances in functional and structural MR image analysis and implementation as FSL. *Neuroimage.* 2004; 23 Suppl 1:S208–219. [PubMed: 15501092]
41. Woolrich MW, Jbabdi S, Patenaude B, Chappell M, Makni S, Behrens T, et al. Bayesian analysis of neuroimaging data in FSL. *Neuroimage.* 2009; 45(1 Suppl):S173–186. [PubMed: 19059349]
42. Zhang Y, Brady M, Smith S. Segmentation of brain MR images through a hidden Markov random field model and the expectation-maximization algorithm. *IEEE Trans Med Imaging.* 2001; 20(1): 45–57. [PubMed: 11293691]
43. Herringa RJ, Birn RM, Ruttle PL, Burghy CA, Stodola DE, Davidson RJ, et al. Childhood maltreatment is associated with altered fear circuitry and increased internalizing symptoms by late adolescence. *Proc Natl Acad Sci U S A.* 2013
44. Burghy CA, Stodola DE, Ruttle PL, Molloy EK, Armstrong JM, Oler JA, et al. Developmental pathways to amygdala-prefrontal function and internalizing symptoms in adolescence. *Nat Neurosci.* 2012; 15:1736–1741. [PubMed: 23143517]
45. MacKinnon DP, Lockwood CM, Hoffman JM, West SG, Sheets V. A comparison of methods to test mediation and other intervening variable effects. *Psychol Methods.* 2002; 7:83–104. [PubMed: 11928892]
46. Baron RM, Kenny DA. The moderator-mediator variable distinction in social psychological research: Conceptual, strategic, and statistical considerations. *J Pers Soc Psychol.* 1986; 51:1173–1182. [PubMed: 3806354]
47. Lim SL, Padmala S, Pessoa L. Segregating the significant from the mundane on a moment-to-moment basis via direct and indirect amygdala contributions. *Proc Natl Acad Sci U S A.* 2009; 106:16841–16846. [PubMed: 19805383]
48. Wager TD, Davidson ML, Hughes BL, Lindquist MA, Ochsner KN. Prefrontal-subcortical pathways mediating successful emotion regulation. *Neuron.* 2008; 59:buhle1037–1050.
49. Shackman JE, Shackman AJ, Pollak SD. Physical abuse amplifies attention to threat and increases anxiety in children. *Emotion.* 2007; 7:838–852. [PubMed: 18039053]
50. Clogg CC, Petkova E, Shihadeh ES. Statistical methods for analyzing collapsibility in regression models. *Journal of Educational Statistics.* 1992; 17:51–74.
51. Barbas H, De Olmos J. Projections from the amygdala to basoventral and mediodorsal prefrontal regions in the rhesus monkey. *J Comp Neurol.* 1990; 300(4):549–571. [PubMed: 2273093]
52. Amaral DG, Insausti R. Retrograde transport of D-[3H]-aspartate injected into the monkey amygdaloid complex. *Exp Brain Res.* 1992; 88(2):375–388. [PubMed: 1374347]
53. Amaral DG, Price JL. Amygdalo-cortical projections in the monkey (*Macaca fascicularis*). *J Comp Neurol.* 1984; 230(4):465–496. [PubMed: 6520247]
54. Miller EK, Cohen JD. An integrative theory of prefrontal cortex function. *Annu Rev Neurosci.* 2001; 24:167–202. [PubMed: 11283309]
55. Shackman AJ, McMenamin BW, Maxwell JS, Greischar LL, Davidson RJ. Right dorsolateral prefrontal cortical activity and behavioral inhibition. *Psychological Science.* 2009; 20:1500–1506. [PubMed: 19906125]
56. Koenigs M, Huey ED, Calamia M, Raymont V, Tranel D, Grafman J. Distinct regions of prefrontal cortex mediate resistance and vulnerability to depression. *J Neurosci.* 2008; 28:12341–12348. [PubMed: 19020027]

57. Ekstrom LB, Roelfsema PR, Arsenault JT, Kolster H, Vanduffel W. Modulation of the contrast response function by electrical microstimulation of the macaque frontal eye field. *J Neurosci*. 2009; 29:10683–10694. [PubMed: 19710320]
58. Premereur E, Janssen P, Vanduffel W. FEF-microstimulation causes task-dependent modulation of occipital fMRI activity. *Neuroimage*. 2012; 67:42–50. [PubMed: 23186918]
59. Pezawas L, Meyer-Lindenberg A, Drabant EM, Verchinski BA, Munoz KE, Kolachana BS, et al. 5-HTTLPR polymorphism impacts human cingulate-amygdala interactions: a genetic susceptibility mechanism for depression. *Nat Neurosci*. 2005; 8:828–834. [PubMed: 15880108]
60. Kim MJ, Gee DG, Loucks RA, Davis FC, Whalen PJ. Anxiety dissociates dorsal and ventral medial prefrontal cortex functional connectivity with the amygdala at rest. *Cereb Cortex*. 2011; 7:1667–1673. [PubMed: 21127016]
61. Akam T, Kullmann DM. Oscillatory multiplexing of population codes for selective communication in the mammalian brain. *Nat Rev Neurosci*. 2014; 15:111–122. [PubMed: 24434912]
62. Cabral J, Kringelbach ML, Deco G. Exploring the network dynamics underlying brain activity during rest. *Prog Neurobiol*. 2014; 114C:102–131. [PubMed: 24389385]
63. Logothetis NK. What we can do and what we cannot do with fMRI. *Nature*. 2008; 453:869–878. [PubMed: 18548064]
64. Arnsten AF. Stress signalling pathways that impair prefrontal cortex structure and function. *Nat Rev Neurosci*. 2009; 10:410–422. [PubMed: 19455173]
65. Shackman AJ, Maxwell JS, McMenemy BW, Greischar LL, Davidson RJ. Stress potentiates early and attenuates late stages of visual processing. *J Neurosci*. 2011; 31:1156–1161. [PubMed: 21248140]
66. Davis M, Whalen PJ. The amygdala: vigilance and emotion. *Mol Psychiatry*. 2001; 6:13–34. [PubMed: 11244481]
67. Fudge JL, Haber SN. The central nucleus of the amygdala projection to dopamine subpopulations in primates. *Neuroscience*. 2000; 97:479–494. [PubMed: 10828531]
68. Fornito A, Harrison BJ, Goodby E, Dean A, Ooi C, Nathan PJ, et al. Functional dysconnectivity of corticostriatal circuitry as a risk phenotype for psychosis. *JAMA Psychiatry*. 2013; 70(11):1143–1151. [PubMed: 24005188]
69. Guller Y, Ferrarelli F, Shackman AJ, Sarasso S, Peterson MJ, Langheim FJ, et al. Probing thalamic integrity in schizophrenia using concurrent transcranial magnetic stimulation and functional magnetic resonance imaging. *Arch Gen Psychiatry*. 2012; 69(7):662–671. [PubMed: 22393203]
70. Chen AC, Oathes DJ, Chang C, Bradley T, Zhou ZW, Williams LM, et al. Causal interactions between fronto-parietal central executive and default-mode networks in humans. *Proc Natl Acad Sci U S A*. 2013; 110(49):19944–19949. [PubMed: 24248372]
71. Bullmore E. The future of functional MRI in clinical medicine. *Neuroimage*. 2012; 62(2):1267–1271. [PubMed: 22261374]
72. Button KS, Ioannidis JP, Mokrysz C, Nosek BA, Flint J, Robinson ES, et al. Power failure: why small sample size undermines the reliability of neuroscience. *Nat Rev Neurosci*. 2013; 14(5):365–376. [PubMed: 23571845]
73. Davidson RJ. Affective style and affective disorders: Perspectives from affective neuroscience. *Cognition & Emotion*. 1998; 12:307–330.
74. Badre D, D'Esposito M. Is the rostro-caudal axis of the frontal lobe hierarchical? *Nat Rev Neurosci*. 2009; 10:659–669. [PubMed: 19672274]

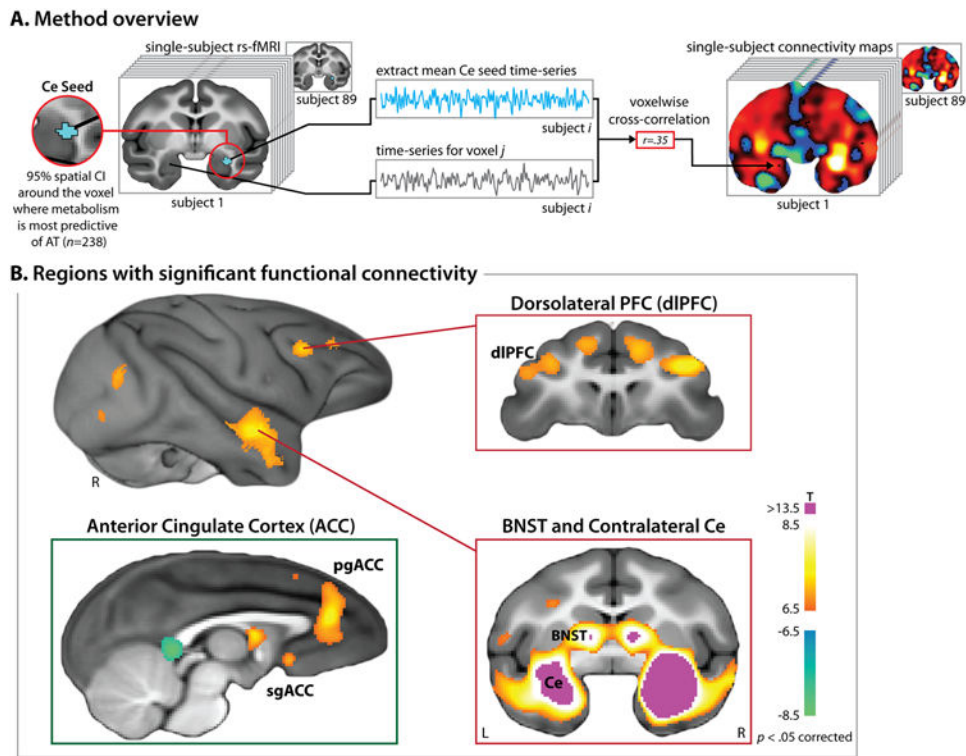


**Fig. 1. Intrinsic functional connectivity of the central nucleus (Ce) of the amygdala in young monkeys**

**A. Method overview.** The seed for functional connectivity analyses (depicted in turquoise) was functionally defined as the 95% spatial confidence interval (CI) surrounding the Ce voxel where FDG metabolism best predicted individual differences in anxious temperament (AT) in a superset of 238 individuals (detailed in Ref. <sup>12</sup>). Using the mean de-noised echoplanar imaging (EPI) time-series from the seed (see the Method and SI), we computed voxelwise estimates of the strength of functional connectivity for each of the 89 individuals.

**B. Regions with significant functional connectivity with the Ce.** Significant ( $p < .05$ , corrected) clusters included the dorsolateral prefrontal cortex (dlPFC), pregenual anterior cingulate cortex (pgACC), subgenual ACC (sgACC), bed nucleus of the stria terminalis (BNST), and contralateral Ce. Red lines indicate the locations of the two coronal slices.

**Abbreviations**—**L**: left hemisphere; **R**: right hemisphere.

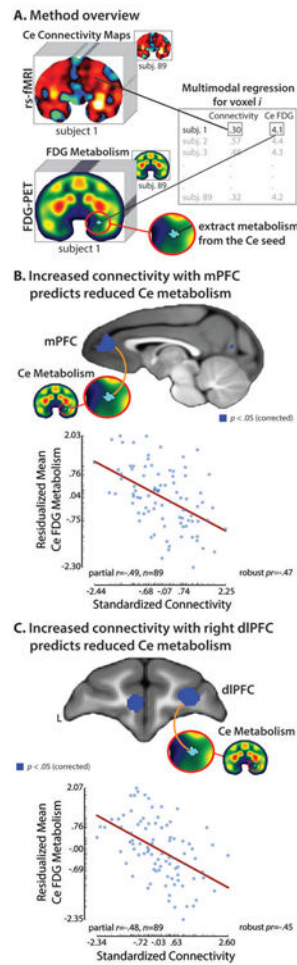


**Fig. 2. Prefrontal cortex (PFC)-Ce intrinsic functional connectivity predicts Ce metabolism in young monkeys**

**A. Method overview.** For each monkey, a Ce functional connectivity map was computed and the mean level of FDG metabolism was extracted from the Ce seed (turquoise region). Individual differences in Ce metabolism were used to predict voxelwise functional connectivity with the Ce throughout the brain. **B. Decreased functional connectivity with the medial PFC (mPFC) predicts increased Ce metabolism.** **C. Decreased functional connectivity with the right dorsolateral PFC (dIPFC) predicts increased Ce metabolism.** For illustrative purposes, scatter plots depict the partial correlations between connectivity and metabolism for the cluster averages. Axis labels indicate the minimum, maximum, and interquartile range. Partial correlation coefficients computed using robust regression techniques<sup>11</sup> are shown to the right of each scatter plot.

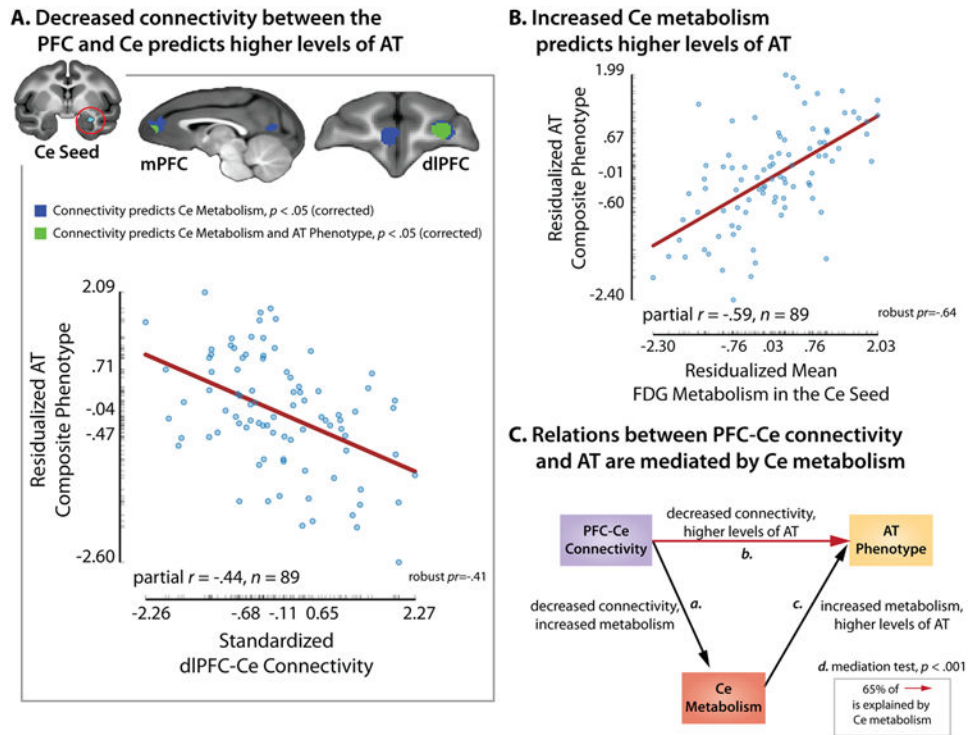


**Fig. 3. Intrinsic functional connectivity between the PFC and Ce predicts individual differences in the AT phenotype in young rhesus monkeys**

**A. Decreased connectivity between the PFC and Ce predicts higher levels of AT.** Upper panel depicts the regions within the mPFC and dlPFC clusters where the strength of functional connectivity significantly predicted variation in both Ce metabolism and AT (displayed in green;  $p < .05$ , corrected). Lower panel shows the partial correlation between dlPFC-Ce connectivity and AT (controlling for age and sex). **B. Increased Ce metabolism predicts higher levels of AT.** **C. Relations between PFC-Ce connectivity and AT are significantly mediated by Ce metabolism.** Summary of the four tests (*a-d*) incorporated in the multivariate mediation framework (see the SI). For scatter plot conventions, see Fig. 3. Panel depicts results for the dlPFC. Similar results were obtained for the mPFC (see Table S4).

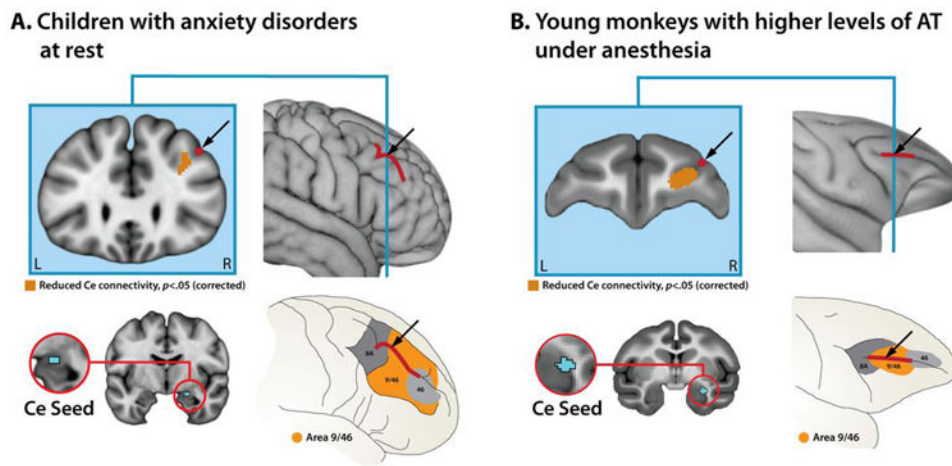


**Fig. 4. Homologous dlPFC subdivisions show decreased intrinsic connectivity with the Ce in anxious children and monkeys**

**A. Children with anxiety disorders at rest.** Bottom-left panel shows the Ce seed (cyan in red ring). Upper-left panel depicts a coronal slice through the human dlPFC cluster (dark orange;  $p < .05$ , corrected for the combined volume of the mPFC and right dlPFC; n.s. when corrected for the volume of the whole brain). The intermediate frontal sulcus (IFS) is shown in dark red. Upper-right panel shows the IFS with the location of the coronal slice indicated by the blue vertical line. Bottom-right panel shows the location of the dlPFC cluster relative to the architectonic subdivisions of the human dlPFC. **B. Young monkeys with high levels of AT under anesthesia.** Conventions are similar to A; dark red indicates the location of the sulcus principalis. The bottom-right panels of this figure were adapted with permission from Ref. <sup>74</sup>.